

3.1 S. Soisuwan, B. Netiworraksa, T. Tubchareon, C. Chareondechanukor, P. Praserthdam, "Reductive Behaviors and H₂ Chemisorption of Cobalt Catalyst Supported ZrO₂-La₂O₃ Mixed Oxide" Oral Presentation, Nanocatalysis : Fundamentals and Application, A Pre-Conference of 14th ICC, Dalian, China , July 9-12, 2008

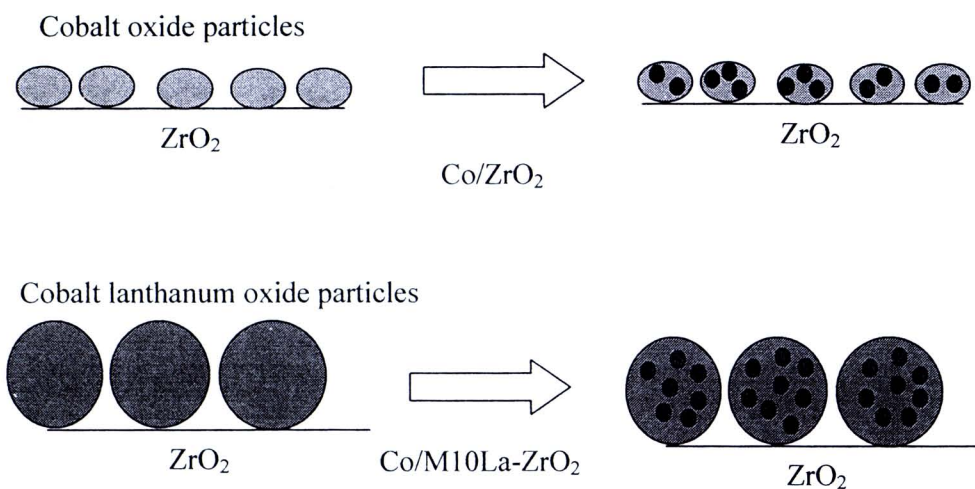
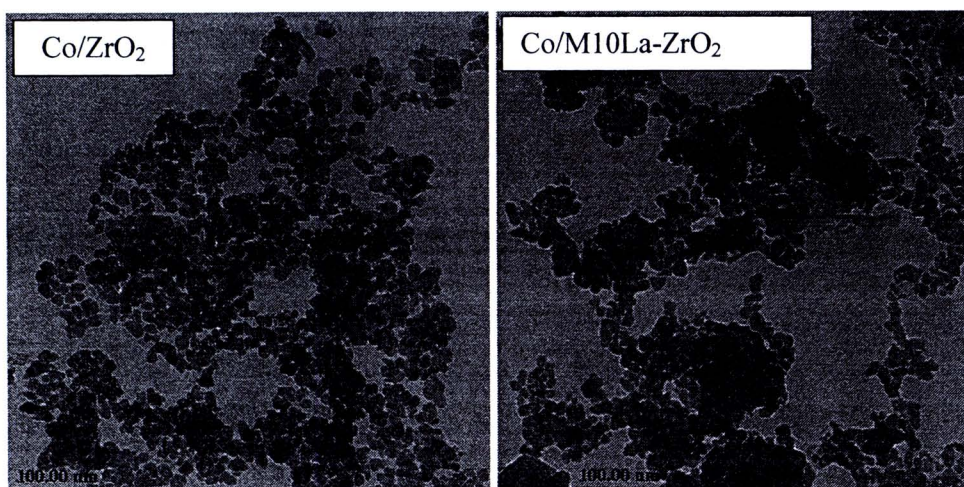
3.2 S. Soisuwan, K. Jiradechkhajorn, S. Prawong, P. Praserthdam, "Catalytic Characterization of ZrO₂ -La₂O₃ Mixed Oxide" Poster Presentation, Nanocatalysis : Fundamentals and Application, A Pre-Conference of 14th ICC, Dalian, China , July 9-12, 2008

บรรณานุกรม

-
- 1 . H.Schulz, Appl. Catal. A 186 (1999) 3.
 2. R.B. Anderson, Fischer-Tropch synthesis, Academic Press, NY, 1984.
 - 3 . M.E. Dry, Catal. Today 71 (2002) 227.
 - 4 . E. Iglesia, S.L. Soled, R.A. Fiato, G.H. Via, J. Catal. 143 (1993) 345.
 - 5 . D. Schanke, S. Vada, E.A. Blekkan, A.M. Hilmen, A. Hoff, A Holmen, J. Catal. 156 (1995) 85.
 6. A. Kogelbauer, J.G. Goodwin, R.J. Oukaci, J. Catal. 160 (1996) 125.
 7. R. Riva, H. Miessner, R. Vitali, G. D. Piero, Appl. Catal. A 196 (2000) 111.
 8. B. Jongsomjit, C. Sakdamnuson, J.G. Goodwin Jr., P. Praserthdam, Catal. Lett. 94 (2004) 209
 9. K.I. Maruya, A. Takasawa, T. Haraoka, K. Domen, T. Onishi, J. Mol. Catal. A 112 (1996) 143
 10. T. Maehashi, K. Maruya, K. Domen, K. Aika, T. Onishi, Chem. Lett. (1984) 747.
 11. H. Abe, K. Maruya, K. Domen, T. Onishi, Chem Lett. (1984) 1875.
 12. Tanabe, K., Mater Chem. Phys., 13 (1985) 347
 13. D. I. Enache, M. Roy-Auberger, R. Revel, Appl. Catal. A: General, 268 (2004) 51
 14. D. I Enache, B. Rebours, M. Roy-Auberger, R. Revel, J. Catal., 205 (2002) 346
 15. J. Panpanot, N. Taochaiyaphum, P. Praserthdam, Mater. Chem. Phys. 94 (2005) 207
 16. A. Feller, M. Claeys, E.V. Steen, J. of Catal., 185 (1999) 120

-
17. G.R. Moradi, M.M. Basir, A. Taeb, Kiennemann, Catal. Comm. 4 (2003) 27
 18. R. Oukaci, A.H. Singletonand, J. Goodwin Jr., Appl. Catal. A: General 186 (1999) 129
 19. S. Kongwudthiti, P. Praserthdam, W. Tanakulrungsank, M. Inoue, J. Mater. Proc. Tech., 136 (2003) 186
 20. S. Soisuwan, Ph. D. Thesis, Chulalongkorn University, (2005)
 21. J.S. Ledford, M. Houalla, A. Proctor, D.M. Hercules, L. Petrakis, J. Phys. Chem, 93 (1989) 6770-6777.
 - 22 . A.Y. Khodakov, W. Chu, F. Pascal, Chem. Rev., 107 (2007) 1692-1744
 - 23 . T. Wang, Y. Ding, Y. Lü, H. Zhu, L. Lin, J. Natur. Gas Chem., 17 (2008) 153-158.
 - 24 . S. Vada, B. Chen, J.G. Goodwin, J. Catal., 153 (1995) 224-231
 25. J.G. Haddad, B. Chen, B., J.G. Goodwin, J. Catal., 161 (1996) 274-281
 - 26 . J. Barrault, A. Guilleminot, Appl. Catal. , 21 (1986) 307-312
 - 27 . L.F. Liotta, G. Di Carlo, A. Longo, G. Pantaleo, G. Deganello, G. Marci, A. Martorana, J. Non-Crytalline Solids, 345&346 (2004) 620-623
 28. P. Thangadurai, V. Sabarinathan, A. Chandra Bose, S. Ramasamy, J. Phys. Chem. Solids, 65 (2004) 1905-1912
 29. J.O. Petunchi, M.A. Ulla, J.A. Marco, E.A. Lombardo, J. Catal. , 70 (1981) 356-363
 30. C.W. Conner, J.L. Falconer, Chem. Rev., 95 (1995) 759-788

Graphical Abstract



After the standard reduction

The presence of lanthana in modified-zirconia support can contribute the agglomeration of cobalt oxide particles as the evident was extremely large cobalt oxide particles/clusters found on the La-modified zirconia supports. The cobalt lanthanum oxide particles/clusters arising from dissolution of lanthana in starting cobalt solution coverage on mechanically mixing support facilitated the ease of reduction and higher reducibility leading to increase of active metal dispersed cobalt atoms and catalytic activity.

Influence of the preparation procedure on physicochemical and catalytic activity of Co/ZrO₂-La₂O₃ catalysts for CO hydrogenation

Soipatta Soisuwan^{1,*}, Benjamas Netiworaksa¹, Chanarong Charoendechanukor¹, Tassanee Tabcharoen¹, Joongjai Panpranot² and Piyasan Praserttham²

¹Department of Chemical Engineering, Faculty of Engineering, Burapha University, 169 Long-Hard Bangsaen Road, Saensuk, Muang, Chonburi, 20131 Thailand

²Center of Excellence on Catalysis and Catalytic Reaction Engineering, Department of Chemical Engineering, Faculty of Engineering, Chulalongkorn University, Bangkok, 10330, Thailand

Abstract

The effect of lanthana-modified zirconia support (10 mol% La), prepared by three different methods i.e. co-precipitation, impregnation and mechanically mixing, on cobalt catalyst characteristics and catalytic activity for CO hydrogenation (CO:H₂ at 1:9) was investigated at atmospheric pressure. Although the lanthana-modified zirconia supported cobalt catalysts possessed surface areas on the narrow range of 40-50 m²/g, the CO adsorption results revealed the highest active metal dispersion over lanthana-modified zirconia supported cobalt catalyst derived from mechanically mixing method (26.47×10^{18} molecules/ g catalyst) compared to the cobalt particles/clusters on La-modified supports derived from other ways. This could be ascribed by the lowest reduction temperature (maximum at 330°C) and the highest reducibility (45%) arising from significant interaction of the support and cobalt lanthanum compound particles/clusters. The catalytic activities of all catalysts were correspondence to the CO chemisorption results. However, the most active catalyst was deactivated within 6-h CO hydrogenation testing.

Keywords; ZrO₂, La₂O₃, mixed oxide support, cobalt catalyst, CO hydrogenation

1. Introduction

The development of active cobalt catalysts for CO hydrogenation and Fischer-Tropsch reaction has been of interest for several years in order to convert the synthetic gases to higher hydrocarbon substituting for the fossil fuel derived from crude oil. In general, the potential commercial cobalt catalysts are typically composed of four components: Co metal, a small amount of second metal, oxide promoters (alkali, rare earth, and/or transition metal oxide such as ZrO_2) and supports (silica, alumina or titania) [1]. Recently, zirconia has been drawn much attention for CO hydrogenation, aside from application as a promoter it was employed as a support materials because of the possession of chemical properties i.e. acidity, basicity, reducing or oxidizing ability and electronic properties leading to significant interaction of cobalt oxide particles/clusters and support [2]. However, pure zirconia support was occasionally found the drawbacks of cobalt-support compound formation and usually low surface areas limiting catalytic phase dispersion [3], so as to it may not be suitable to employ as the sole support and the modification of zirconia would be necessary. The metal-modified zirconia or zirconia mixed oxide supports have been currently investigated for cobalt catalysts such as $Al_2O_3-ZrO_2$ [4], SiO_2-ZrO_2 [5], B-modified ZrO_2 [18] and the consensus was that their synergetic effects can give a significant change of metal-support interaction and rise to higher catalytic activity by small quantity of second oxide modification. The lanthana, one of interesting rare earth promoters for cobalt catalyst, was reported to be beneficial for CO hydrogenation to produce long chain hydrocarbon and it showed a significant enhancement of catalytic activity owing to increase of active site dispersion [6-11]. The synergetic effect of both lanthana and zirconia was applied as cobalt catalyst supports in the present study. In order to alter electronic properties of lanthana and zirconia mixed oxides, the support preparation was divided into 3 different routes i.e. i) co-precipitation, ii) impregnation and iii)



mechanically mixing. The effect of La-modification of zirconia on the characteristics and catalytic properties of zirconia-supported cobalt catalyst during CO hydrogenation was investigated by various techniques.

2. Experimental

2.1 Catalyst Preparation

2.1.1 La-modified ZrO₂ support

The mixed oxide supports were prepared by three different methods i.e. i) co-precipitation, ii) impregnation and iii) mechanical mixing. The zirconia support composed of La³⁺ 10% on molar basis that was synthesized via a pH precipitation technique was given a name of P10La₂O₃-ZrO₂. In brief, a mixed aqueous solution of zirconyl nitrate [ZrO(NO₃)₂.~xH₂O] (Aldrich) and lanthanum nitrate [La(NO₃)₃.6H₂O] (Aldrich) was co-precipitated with ammonium hydroxide solution (NH₃ solution) at room temperature to achieve pH = 9 before 1-day aging. The precipitate separated centrifugally from its supernatant was dried at 110°C for 24 h and then calcined under atmospheric air at 600°C for 6 h. The lanthana coverage on zirconia support was namely I10La-ZrO₂. The 1-day drying of as-precipitated zirconium hydroxide was carried out at 110 °C in order to remove moisture prior to impregnation of La³⁺ starting solution at atomic ratio of La³⁺/Zr⁴⁺ =1:9. The calcination was operated at 600°C under atmospheric oxygen for 6 h. M10La-ZrO₂ was assigned to the lanthana and zirconia mixed oxide support prepared by mechanically mixing. The lanthana and zirconia were separately prepared. The precipitation of lanthanum hydroxide took place at pH equal to 7 as then following the steps of oxide preparation i.e. i) 1-day drying at 110 °C and ii) calcination at 600°C. Both oxides were mechanically mixed at the same atomic ratio as impregnation and co-precipitation routes.

2.1.2 The La-modified zirconia supported cobalt catalysts.

The 10 wt% cobalt metal supported on the mixed oxide was prepared by incipient wetness impregnation. The resulting samples were dried at 110°C for 12 h and calcined in air at 350°C for 3 h. All samples are named as Co/P10La₂O₃-ZrO₂, Co/I10La₂O₃-ZrO₂ and Co/M10La₂O₃-ZrO₂, respectively. The cobalt catalysts supported on pure ZrO₂ and pure La₂O₃, namely Co/ZrO₂ and Co/La₂O₃, were prepared in comparison with the mixed oxide supported catalysts.

2.2 Catalyst Characterization

2.2.1 BET surface area

The N₂ physisorption at 77K was performed in Quantachorm 1996 model NOVA 1200 automated system to determine the multiple point BET surface area. The experiment was carried out in the range of P/P₀ from 0.05 to 0.35. A 500-mg sample was degassed under vacuum atmosphere at 300°C held there for 3 h to remove physically adsorbed gas.

2.2.2 X-ray diffraction

The bulk crystalline phase of all samples was determined by a SIEMEN D-5000 X-ray diffractometer with Cu K_α ($\lambda = 1.54439 \text{ \AA}$) at spectra scanning rate of 2.0°/min. The X-ray diffraction spectra were detected in the range of $2\theta = 20\text{-}80^\circ$.

2.2.3 Temperature programmed reduction

The reduction behavior was conducted by temperature-programmed reduction (TPR). The TPR method considers reduction under 5% hydrogen in argon flow up to 800°C ramping at 10°C/min with catalyst 100 mg. The method was carried out by a Micromeritics ASAP 2010. During the reduction, water was removed by a cold trap prior to reading TCD signal.

2.2.4 CO Chemisorption

The number of active cobalt metal sites was determined by CO chemisorption described by Reuel and Bartholomew [26]. Prior to the chemisorption testing, the sample was reduced at 350°C under flowing H₂ for 6 h. The chemisorption of static CO gas was performed at room temperature in a Micromeritics ASAP 2010 and the amount of adsorbed CO was calculated by 2010C V3.00 software.

2.2.5 Scanning Electron Microscopy (SEM) and Energy Dispersive X-ray Spectroscopy (EDX)

The catalyst morphology and elemental distribution was investigated by a Hitachi S-3500N scanning electron microscopy (SEM) operating with the back scattering electron (BSE) mode at 20 kV and the EDX was performed to obtain the elemental analysis on catalyst granules using INCA software.

2.2.6 Transmission Electron Microscopy

The cobalt oxide particles/clusters size distribution was investigated by a JEOL-TEM 200CX transmission electron microscopy operated at 200 kV with 25k magnification.

2.3 CO hydrogenation testing

The catalyst 0.1 g was typically in situ reduced in flowing hydrogen at 350°C for 2 h and then the CO hydrogenation was carried out at CO/H₂/Ar flowing rate of 4/36/20 cm³/min. The effluent gas was taken at 1 h interval and the gas compositions were analyzed by on-line gas chromatography Varian model CP-3800 equipped with consecutive detectors i.e. thermal conductivity and then flame-ionized detectors and it was complicatedly equipped with 30% DC on CPAW and OV 101 columns.

3. Results and discussion

3.1 BET surface area measurement and X-ray powder Diffraction

The present study aims to observe the effect of La-modified zirconia supports and the routes of their preparation on cobalt catalysts for CO hydrogenation. Table 1 lists the results of BET surface areas, crystalline structure and cobalt oxide crystalline sized measured by the X-ray diffraction and determined by Scherrer's equation. The surface areas of catalysts with La modification of zirconia supports increase in the range of 40 to 50 m²/g various upon the methods of preparation i.e. co-precipitation, impregnation, and mechanically mixing. It would notice that the BET surface areas of the catalysts were improved by existing lanthana in zirconia oxide structures. The X-ray diffraction patterns of the cobalt catalysts supported by La₂O₃ – ZrO₂ mixed oxides synthesized in different ways are shown in Figure 1. The crystallographic structure of zirconia remained apparently after impregnation of cobalt nitrate precursor solution and then calcination. The lanthana derived from precipitation possessed a diffraction pattern which could identify as non-crystalline or amorphous form and it was identical after preparation as supported cobalt catalyst. The sharp peaks of tetragonal form appeared at 2θ 29.8°, 34.2°, 49.6° and 59.6° coincidentally with the strong peaks of monoclinic form in X-ray diffraction pattern, at 2θ = 28.2°, 31.5°, 41.0° and 55.8°, of the unmodified zirconia support, whereas only the strong peak of tetragonal phase consisted apparently in the La-modified zirconia support prepared by the co-precipitation and the impregnation. The existence of La seems to induce formation of tetragonal structure rather than being as monoclinic form. These tetragonal structures may arise from the incorporation of La³⁺ ion to zirconium oxide structures as impurity or structural defect which could thermodynamically stimulate the formation of meta-stable tetragonal zirconia existing at unusual temperature [12]. The crystal sizes determined by Scherrer's equation at tetragonal main peak (111) or 2θ = 29.8° were in the range of 10-12 nm. A slight shift in tetragonal main peak was observed

towards the low diffraction angle indicating the substitution of the larger La^{3+} ion into the ZrO_2 lattice as mentioned by Thangadurai et al. [13]. The La-incorporated tetragonal ZrO_2 possessed the crystalline size in a minor difference with the pure tetragonal ZrO_2 despite consisting of larger ionic radius as La^{3+} ions. The presence of Co_3O_4 was determined by the X-ray diffraction positioned at 36° , 45° , 60° (overlap with the X-ray diffraction of tetragonal zirconia) and 65° which was marked by their indices planes (311), (400), (511) and (440) of the face-center cubic (fcc) cobalt oxide [14,15]. The absence of X-ray diffraction peak was found in the lanthana-supported cobalt catalyst even though cobalt loading was as high as 10% indicating that cobalt oxide would exist in a non-detectable crystalline form which was smaller than the limitation of X-ray diffraction or the well dispersed cobalt oxide would occur in amorphous form. The crystal sizes of supported cobalt oxide calculated by Scherrer's equation using the main peak of (311) were ranged from 5 to 16 nm as shown in Table 1. It should note that the crystalline cobalt oxide species on I10La-ZrO_2 support inspected by X-ray diffraction appeared only at $2\theta = 36^\circ$ (311) by which the crystalline structure seems to be imperfectly aligned, indicating as imperfect crystalline cobalt oxide or amorphous species.

3.2 SEM and EDX mapping and TEM micrographs

The SEM and EDX were performed in order to investigate morphologies and element distribution of the catalyst in Figure 2. It would notice that cobalt element appears to have been agglomerated well on the La-modified zirconia supports as the EDX mapping of cobalt distribution was observed densely on their catalyst granules, while the weakly agglomeration was illustrated on Co/ZrO_2 and $\text{Co/La}_2\text{O}_3$. Moreover, it was found that La element was distributed well all over the La-modified ZrO_2 granule and the La/Zr atomic ratio based on EDX mapping results were approximately at 15:85 for co-precipitation and impregnation and at 10:90 for mechanically mixing method. Moreover, the high resolution TEM was

employed in order to deeply investigate the crystalline size and cobalt oxide dispersion. The TEM micrographs of all the supported cobalt catalysts were shown in Figure 3. There were significant changes in the catalyst morphologies dependently on the support preparations and the presence of La. It should note that ZrO_2 particles illustrated by TEM gave the average size in the range of 10-20 nm slightly close to crystal sizes (10-12 nm) calculated by Scherrer's equation for Co/ZrO_2 and $Co/M10La-ZrO_2$. According to TEM, the good dispersion of cobalt oxide species was found on pure zirconia support leading to smaller size of cobalt oxide particles (~17 nm), while larger cobalt oxide species were obviously observed on the La-modified zirconia support i.e. $Co/P10La-ZrO_2$ (~132 nm), $Co/I10La-ZrO_2$ (~160 nm), and $Co/M10La-ZrO_2$ (~124 nm) arising from the poorly thermal distribution over the mixed oxide. It may say that the presence of La on zirconia support has an effect on agglomeration of cobalt oxide species. The metal dispersion investigated by TEM was in agreement with the element distribution of EDX mapping. There was none of crystalline particle, which would be very small or weakly agglomerated, observed on lanthana supports corresponding to the X-ray diffraction result. However, the crystalline sizes of cobalt oxide obtained by TEM and X-ray diffraction were different obviously in an order of magnitude. This was because of the agglomeration of primary particles into secondary particles as seen by TEM micrographs [16].

3.3 Temperature programmed reduction and CO chemisorption

The temperature programmed reduction was performed in order to determine the reduction behavior of all catalysts. The TPR profiles of the cobalt oxide catalysts supported by various types of La-modified zirconia prepared in different ways compared with those of Co/ZrO_2 and Co/La_2O_3 are shown in Figure 4 and the reduction temperature are listed in Table 2. The cobalt oxide crystalline particles deposited on various types of La-modified

zirconia supports were supposed to be Co_3O_4 for all catalysts according to the X-ray diffraction. The spinel Co_3O_4 basically constitutes of unstable Co_2O_3 and stable CoO phases which are generally reduced in two steps i.e. i) $\text{Co}_3\text{O}_4 + \text{H}_2 \rightarrow 3\text{CoO} + \text{H}_2\text{O}$ and then ii) $3\text{CoO} + 3\text{H}_2 \rightarrow 3\text{Co} + 3\text{H}_2\text{O}$. The appearance of two-step reduction peaks may or may not be observed usually upon the temperature programmed conditions and the reduction temperature of unsupported cobalt oxide species was reported approximately around 300 – 350 °C [17]. The TPR profiles of all catalysts in this study showed the overlap peak of two-step reductions and the first of reduction peaks occurred at temperature 300°C or lower except $\text{Co/La}_2\text{O}_3$. Regarding to the previous section, the presence of 10-mol% La could activate the agglomeration of primary cobalt oxide to be larger secondary particles and these particles were easily reduced to metal atoms at low reduction temperature owing to decrease in metal-support interaction as described by Jongsomjit B. et al. [18-20]. However, the reduction of $\text{Co/La}_2\text{O}_3$ occurred at higher reduction temperature may be caused by strong interaction of cobalt oxide particles and lanthana-dominated support which affected the cobalt oxide hardly to be reduced into active cobalt metal atoms. Usually, the chemical stability of lanthanum oxide is insufficient, it can react with water and carbon dioxide in air to form hydroxide and carbonate species [21,22], lanthanum oxide would degrade to be LaO(OH) during the catalyst preparation and subsequently the cobalt lanthanum compound would occur. It is suggested that the compound would be in ABO_3 formula with or without small crystalline perovskite structure or exist in amorphous form after calcination. The reduction temperature and degree of reducibility of Co_3O_4 not only depend upon particle sizes and morphologies caused by different pretreatment conditions [23], but the intrinsic property of supports and metal loading also have influence on ability of cobalt catalyst to undergo the reduction [24,25]. The temperature programmed reduction profiles exhibited the difference in catalyst reduction behaviors of Co/ZrO_2 and cobalt catalyst supported by ZrO_2 -

La₂O₃ mixed oxides as shown in Figure 4 according to change in the interaction of cobalt oxide particles and supports arising from the synergy of ZrO₂ and La₂O₃ properties and their distinctive preparations. The intimate interaction of cobalt oxide species on I1025-ZrO₂, P1025-ZrO₂ or ZrO₂ supports may contribute to lower their reduction degree to the range of 12-18%, whereas the relatively high consumption of hydrogen was observed during the standard reduction of Co/La₂O₃ resulting in the higher reduction degree as shown in Table 2 and it would be ascribed by the reduction of lanthanum cobalt oxide i.e. LaCoO₃ to LaCoO_{3-x} where appears to have been reduced at 300 to 520°C in accordance with the results of Petunchi J.O. et al. [26].



$$x = 1.5 \equiv 3 \text{ electrons } (e) / \text{molecule}$$

However, it should remind that the standard reduction prior to the reaction were different from the temperature programmed reduction conditions and the cobalt metal (Co⁰) is known to be an active phase of cobalt catalyst for CO hydrogenation. Thus, in order to determine the number of active cobalt metal atoms after standard reduction the CO chemisorption was essentially performed since it is significantly corresponded to the overall catalytic activity during CO hydrogenation. The CO adsorption results were exhibited in Table 2 indicating that Co/M10La-ZrO₂ would be the most active catalyst due to possession of the relatively high number of active cobalt metal atoms as it had high reducibility and low reduction temperature amongst the other catalysts. The CO chemisorption results could emphasize the influence of support preparations and presence of lanthana on active site dispersion for CO reactant.

3.4 CO hydrogenation

The activity and selectivity of all catalyst were measured by CO hydrogenation. The reaction study results are shown in Table 4 and Figure 5. The Co/M10La-ZrO₂ catalyst had the highest CO conversion in comparison with the others which are in accordance with the active site dispersion and CO adsorption results. It is obvious that the catalytic activity dramatically depended on i) type of starting cobalt oxide species obtained by distinctive ways of support preparation, ii) cobalt oxide particle sizes and iii) metal-support interaction. According to the previous results i.e. XRD, TEM, TPR and CO chemisorptions, the cobalt oxide species in this study were suspected to be i) entirely cobalt oxide particles on zirconia or P10La-ZrO₂ or I10La-ZrO₂ support, ii) cobalt lanthanum oxide particles (the Co-rich compound) on M10La-ZrO₂ support and iii) cobalt lanthanum oxide particles (the La-rich compound) on La₂O₃ supports. The results would suggest that the appearance of lanthana in a majority of cobalt oxide species could assist the reduction of cobalt oxide giving the higher number of cobalt metal surface atoms to catalyze the reaction. This is in good agreement with Haddad G.J. et al [10]. However, it should be carefully noted that lanthana consisting in zirconia supports such as P10La-ZrO₂ and I10La-ZrO₂ can give the intimate interaction with cobalt oxide particles resulting in lower the reducibility leading to low active cobalt metal atom dispersion and poor catalytic activity, respectively. Inversely, Co/La₂O₃, the La-rich catalyst, exhibited the highest reduction degree, but it gave the lowest active site dispersion and poor catalytic activity because after standard reduction it would be composed of another inactive species of cobalt oxide such as LaCoO_{3-x} as mentioned by Ledford J.S. et al. [6]. It was interesting to note that the rate decreased under 6-hours hydrogenation for the most active Co/M10La-ZrO₂, whereas more enduring hydrogenation was found over the less active Co/ZrO₂, Co/P10La-ZrO₂ and Co/I10La-ZrO₂. It may suggest that the loss of catalytic activity could be ascribed by disappearance of cobalt metal atoms existing amongst cobalt lanthanum

compound on M10La-ZrO₂ - probably with a cause of simple re-oxidation during CO hydrogenation. Considering the product selectivity upon CO hydrogenation as seen in Table 3, the product of methane was predominantly found at 80-90% for all catalysts except for Co/P10La-ZrO₂ and Co/I10La-ZrO₂. The low hydrogenation activity can cause the most formation of higher linear hydrocarbon. The turnover frequency values based on CO adsorption for all catalysts in the range of 0.0003 - 0.0624 sec⁻¹ are shown in Table 3.

4. Conclusions

The presence of lanthana in modified-zirconia support can contribute the agglomeration of cobalt oxide particles as the evident was extremely large cobalt oxide particles/clusters found on the La-modified zirconia supports. However, the result suggested that the effect of lanthana-modified zirconia supports on the hydrogenation activity can be divided into 2 categories dependently on the support preparation procedures. The lanthana consisting mainly in zirconia supports in case of impregnation and co-precipitation gave the intimate interaction of cobalt oxide particles/clusters and supports suppressing the reduction behavior and subsequently resulted in lower reducibility and poorly dispersed active cobalt atoms, whereas the cobalt lanthanum oxide particles/clusters arising from dissolution of lanthana in starting cobalt solution coverage on mechanically mixing support facilitated the ease of reduction and higher reducibility leading to increase of active metal dispersed cobalt atoms and catalytic activity.

Acknowledgements

We would like to thank the financial support from Thailand Research Funding for MRG4980191, Center of Excellence on Catalysis and Catalytic Reaction Engineering, Chulalongkorn University and Faculty of Engineering, Burapha University, Thailand.

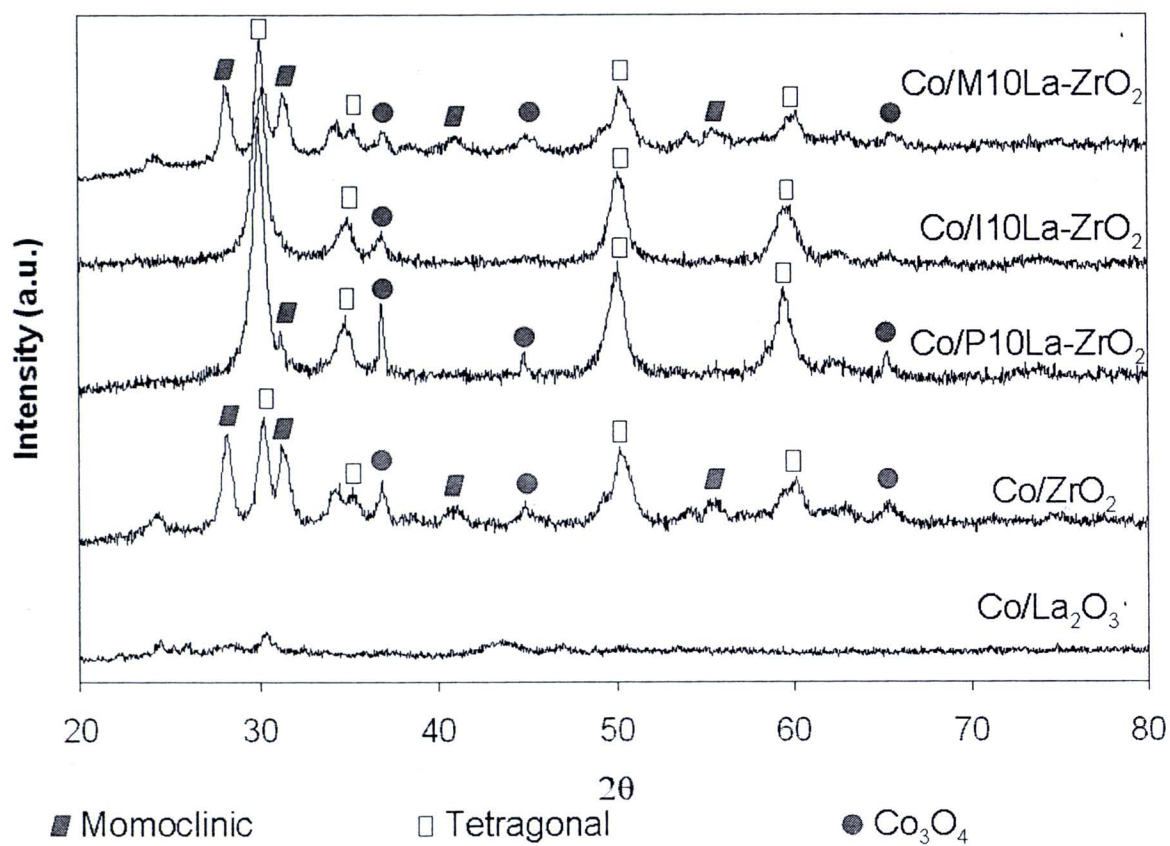


Figure 1 X-ray diffraction patterns of catalyst supported on supports derived from different methods

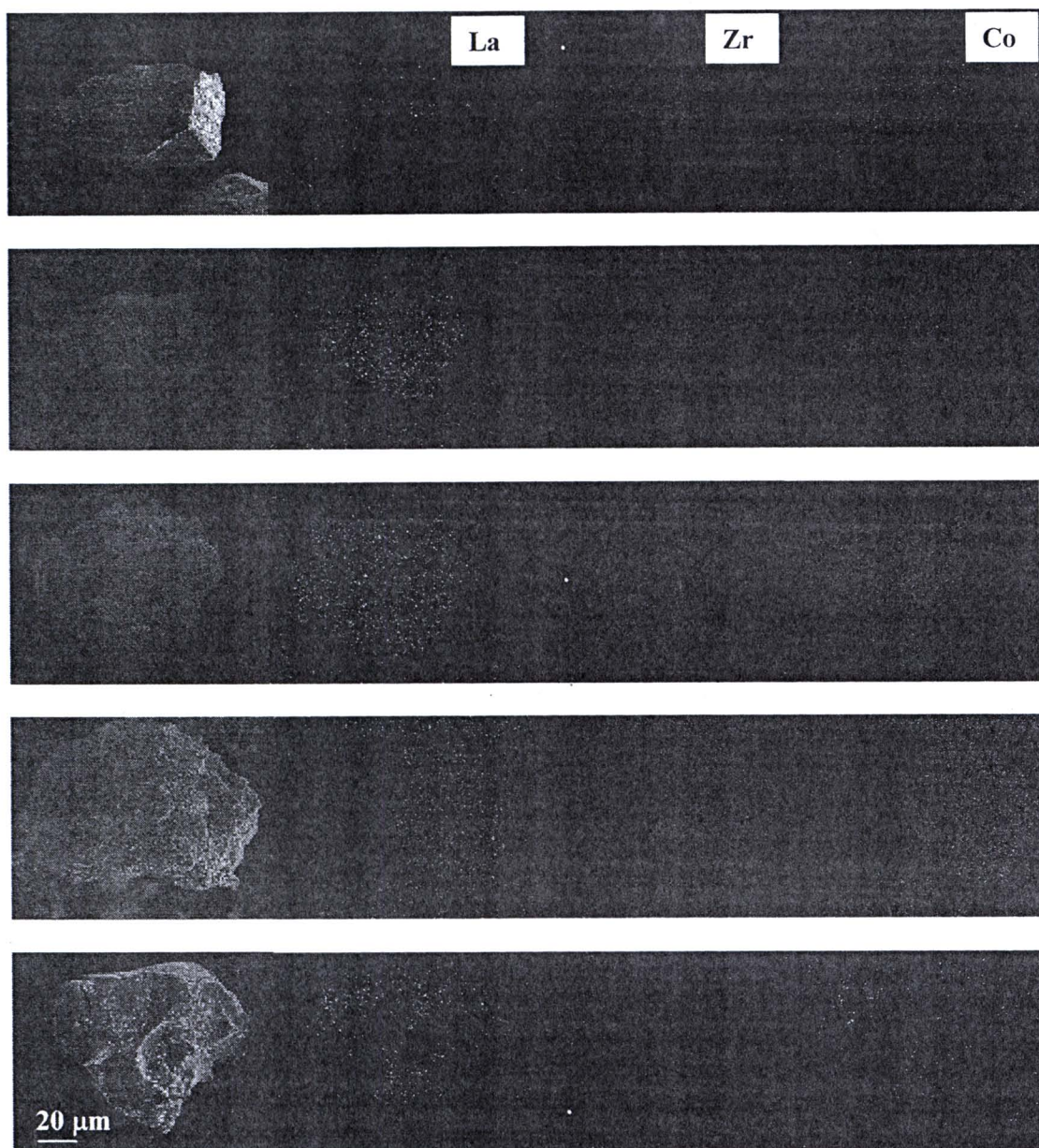


Figure 2 Typical SEM micrographs magnified at $\times 500$ and EDX mapping for Co/ZrO_2 , Co/P10La-ZrO_2 , Co/I10La-ZrO_2 , Co/M10La-ZrO_2 and $\text{Co/La}_2\text{O}_3$.



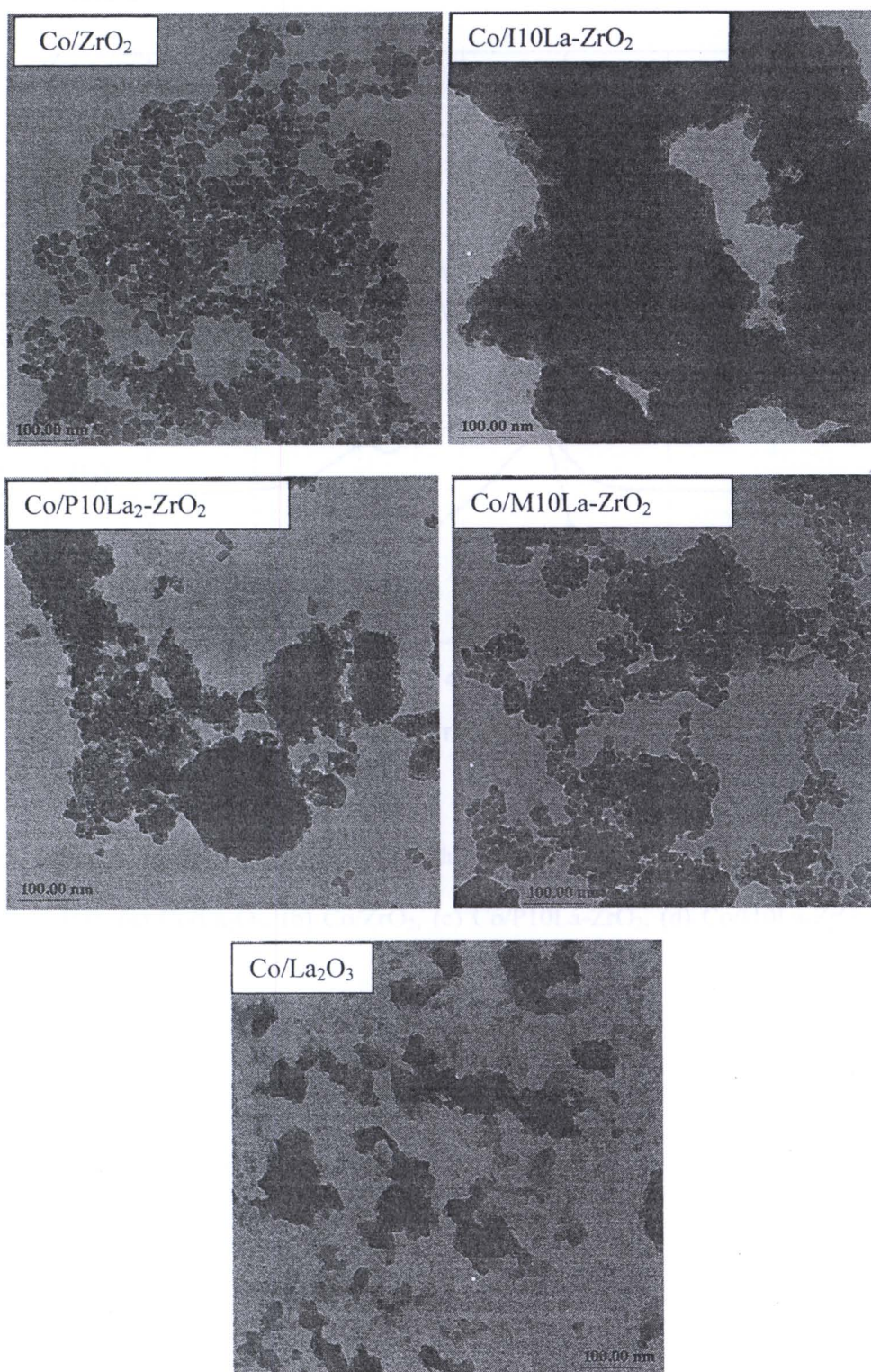


Figure 3 TEM micrographs for different Co/ZrO₂ with 10 wt% of La modification on zirconia support synthesized by different routes and Co/La₂O₃

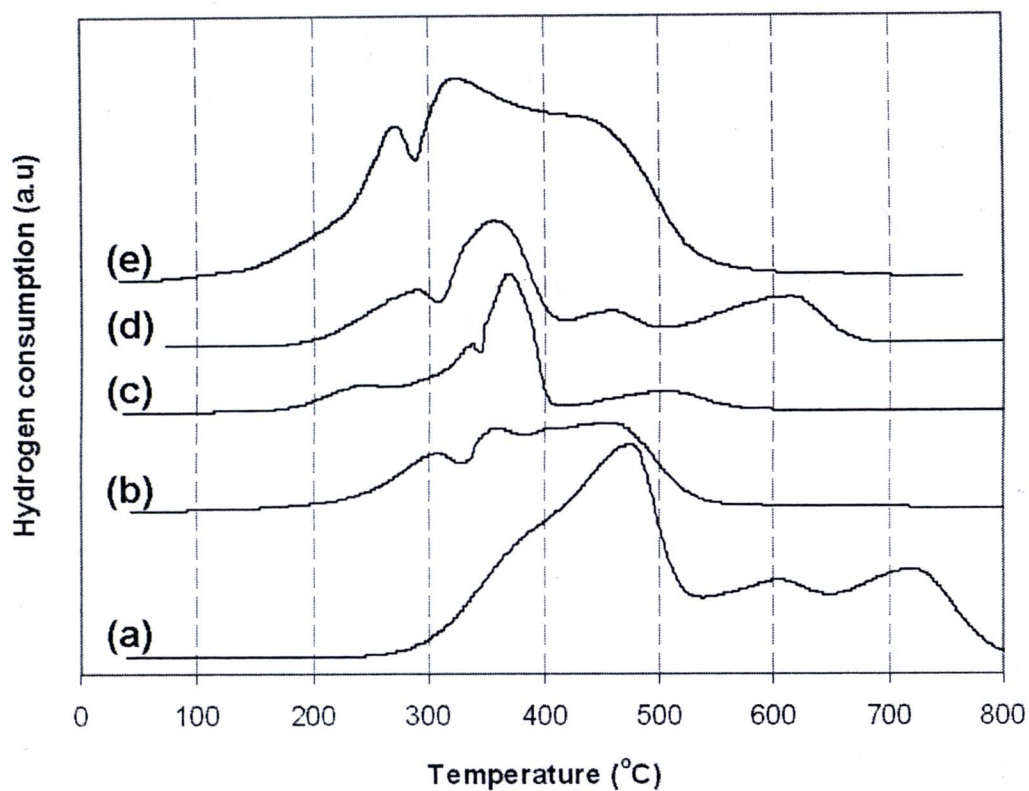


Figure 4 The temperature programmed reduction profiles of different oxides supported cobalt catalyst, (a) Co/La₂O₃, (b) Co/ZrO₂, (c) Co/P10La-ZrO₂, (d) Co/I10La-ZrO₂ and (e) Co/M10La-ZrO₂

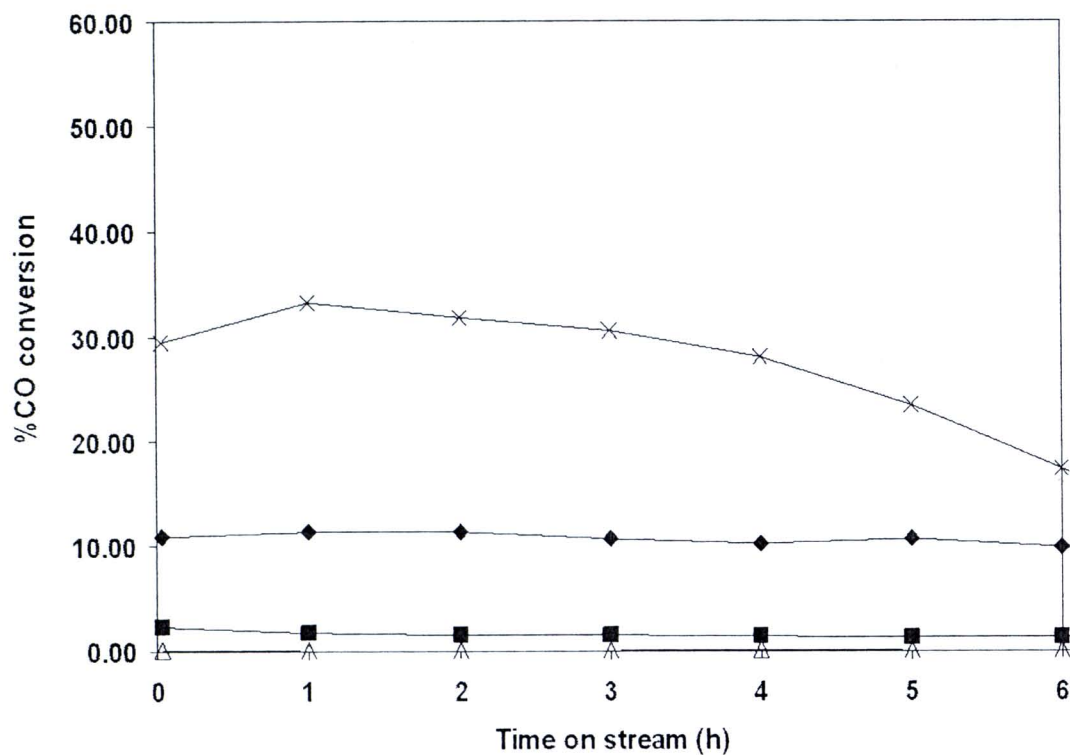


Figure 5 Time on stream for CO hydrogenation of cobalt catalysts on different support preparations; \blacklozenge Co/ZrO₂, \blacksquare Co/P10La-ZrO₂, \triangle Co/H10La-ZrO₂ and \times Co/M10La-ZrO₂

Table 1 Surface area and crystalline phase of Co/La₂O₃-ZrO₂ mixed oxides prepared by different methods

Sample	S _{BET} (m ² /g)	Crystalline Phase		Crystal size of tetragonal ZrO ₂ [*] (nm)	Crystal size of Co ₃ O ₄ [*] (nm)	Average crystalline cobalt oxide diameter (TEM) ^b (nm)
		ZrO ₂	La ₂ O ₃			
Co/ZrO ₂	40	T,M	-	12	6	17
Co/La ₂ O ₃	5	-	A	-	-	-
Co/P10La ₂ O ₃ -ZrO ₂	48	T	A	10	15	132
Co/I10La ₂ O ₃ -ZrO ₂	50	T	A	10	5	160
Co/M10La ₂ O ₃ -ZrO ₂	44	T,M	A	11	8	124

* calculated from Scherer Equation, T: tetragonal, M: monoclinic and A: amorphous

Table 2 Characteristics of Co/La₂O₃-ZrO₂ mixed oxides prepared by different methods

Sample	CO Chemisorption (molecules/ g catalyst) × 10 ¹⁸	% Reducibility	Reduction Temperature (°C)		
			Initial	Final	Maximum
Co/ZrO ₂	11.62	18	200	550	350-450
Co/La ₂ O ₃	0.59	44	380	>800	480
Co/P10La ₂ O ₃ -ZrO ₂	6.27	12	180	610	375
Co/I10La ₂ O ₃ -ZrO ₂	5.10	17	195	690	370
Co/M10La ₂ O ₃ -ZrO ₂	26.47	45	140	580	330

Table 3 Rates of -CH₂- formation on Co/La₂O₃-ZrO₂ mixed oxides prepared by different methods

Sample	TOF (sec ⁻¹)	Rate of -CH ₂ - formation (μmole -CH ₂ - min ⁻¹ g ⁻¹)		% Selectivity at 1 h			% Selectivity at 6 h		
		at 1h	after 6 h	C ₁	C ₂ - C ₃	C ₄₊	C ₁	C ₂ - C ₃	C ₄₊
Co/ZrO ₂	0.0486	56.29	48.86	84.4	12.8	2.8	83.8	13.0	3.2
Co/La ₂ O ₃	0.0000	0.00	0.00	0.0	0.0	0.0	0.0	0.0	0.0
Co/P10La ₂ O ₃ -ZrO ₂	0.0139	8.69	6.03	44.8	24.2	31.0	44.4	25.5	30.1
Co/I10La ₂ O ₃ -ZrO ₂	0.0003	0.14	0.10	43.1	26.8	30.1	29.3	11.9	58.8
Co/M10La ₂ O ₃ -ZrO ₂	0.0624	164.59	85.47	94.6	5.0	0.4	71.3	19.4	9.30

References

- 1 . Haddad G J, Chen B, Goodwin J G (1996) J Catal 274:281.
2. Panpranot J, Tachaiyaphom N, Prasertthdam P (2005) Mater Chem Phys 207:212
- 3 . Enache D I, Roy-Auberger M, Revel R (2004) Appl Catal A : Gen 51:60
- 4 . Soisuwan S, Panpranot J, Trimm D.L., Prasertthdam P. (2006) Appl Catal A: Gen 268:272
- 5 . Jongsomjit B, Womgsalee T, Prasertthdam P, (2006) Mater Chem Phys 343:350
6. Ledford J S, Houalla M, Proctor A, Hercules D M, Petrakis L (1989) J Phys Chem 6770:6777.
7. Khodakov A Y, Chu W, Pascal F (2007) Chem Rev 1692:1744
- 8 . Wang T, Ding Y, Lü Y, Zhu H, Lin L (2008) J Natur Gas Chem 153:158
- 9 . Vada S, Chen B, Goodwin J G (1995) J Catal 224:231
10. Haddad J G, Chen B, Goodwin J G (1996) J Catal 274:281
11. Barrault J, Guilleminot A (1986) Appl Catal 307:312
12. Kelly J R, Denry I (2008) Dent Mater 289:298
13. Thangadurai P, Sabarinathan V, Bose C A, Ramasamy S (2004) J Phys Chem Solids 65 1905:1912
- 14 . Pollard M J, Weinstock B A, Bitterwolf T E, Griffiths P R, Newbery A P, Paine III J B (2008) J Catal 218:225
15. Morsy S M I, Shaban S A, S., Ibrahim A M, Salim M M (2009) J Alloys Comp 83:87
- 16 . Chitpong N, Prasertthdam P, Jongsomjit B (2009) Catal Lett 119:126
17. De la Peña O'Shea V A, Homs N, Pereira E B, Nafria R, Da la Pisca P R (2007) Catal Today 148:152
- 18 . Jongsomjit B, Panpranot J, Goodwin J G (2001) Catal Lett 204: 98
19. Tupabut P, Jongsomjit B, Prasertthdam P (2007) Catal Lett 118:195
- 20 . Panpranot J, Kaewkun S, Prasertthdam P, Goodwin J G (2008) Catal Lett 95:102
21. Nieminen M, Putkonen M, Niinistö L (2001) Appl Surf Sci 155:165
22. De Asha A M, Chritchley J T S, Nix R M (1998) Surf Sci 201:214
23. Potoczna, D, Kepiński L (2001) Catal Lett 41:46
- 24 . Reuel R, Bratholomew C.H. (1984) J Catal 63:77
25. Soisuwan P, Prasertthdam P, Panpranot P, Trimm, D L (2006) Catal Commun 761:767
26. Petunchi, J O, Ulla M A, Marco J A, Lombardo E A (1981) J Catal 356:363



